Activin Receptor-Like Kinase 7 Induces Apoptosis through Up-Regulation of Bax and Down-Regulation of Xiap in Normal and Malignant Ovarian Epithelial Cell Lines

Guoxiong Xu,[1] Hong Zhou,[1] Qinghua Wang,[2] Nelly Auersperg,[3] and Chun Peng[1]

[1]Department of Biology, York University; [2]Departments of Physiology and Medicine, St. Michael's Hospital, University of Toronto, Toronto, Ontario, Canada; and [3]Department of Obstetrics and Gynaecology, University of British Columbia, Vancouver, British Columbia, Canada

Abstract

Transforming growth factor-β superfamily has been implicated in tumorigenesis. We have recently shown that Nodal, a member of transforming growth factor-β superfamily, and its receptor, activin receptor-like kinase 7 (ALK7), inhibit proliferation and induce apoptosis in human epithelial ovarian cancer cell lines. In this study, we further investigated the cellular mechanisms underlying the apoptotic action of ALK7 using an immortalized ovarian surface epithelial cell line, IOSE397, and an epithelial ovarian cancer cell line, OV2008. Infection of these cells with an adenoviral construct carrying constitutively active ALK7 (Ad-ALK7-ca) potently induced cell death; all cells died after 3 and 5 days of Ad-ALK7-ca infection in IOSE397 and OV2008 cells, respectively. ALK7-ca induced the expression of proapoptotic factor Bax but suppressed the expression of antiapoptotic factors Bcl-2, Bcl-X_L, and Xiap. Silencing of Bax by small interfering RNA in IOSE397 cells significantly reduced ALK7-ca-induced apoptosis as measured by terminal deoxynucleotidyl transferase–mediated dUTP nick end labeling assay but partially blocked ALK7-ca-induced caspase-3 activation and did not affect the down-regulation of Xiap by ALK7-ca. Dominant-negative Smad2, Smad3, and Smad4 blocked ALK7-ca-regulated Xiap and Bax expression and caspase-3 activation. Thus, ALK7-induced apoptosis is at least in part through two Smad-dependent pathways, Bax/Bcl-2 and Xiap. (Mol Cancer Res 2006;4(4):235–46)

Received 9/13/05; revised 1/24/06; accepted 2/27/06.
Grant support: Canadian Institutes of Health Research (CIHR) grants MOP 134484 and MOP 93784 (C. Peng) and MOP 57890 (Q. Wang); National Cancer Institute of Canada (N. Auersperg); Ontario Women's Health Scholars Award (G. Xu); and Ontario Premier's Research Excellent Award and Ontario Women's Health Council/CIHR Mid-Career Award (C. Peng).
The costs of publication of this article were defrayed in part by the payment of page charges. This article must therefore be hereby marked advertisement in accordance with 18 U.S.C. Section 1734 solely to indicate this fact.
Requests for reprints: Chun Peng, Department of Biology, York University, 4700 Keel Street, Toronto, Ontario, Canada M3J 1P3. Phone: 416-736-2100; Fax: 416-736-5698. E-mail: cpeng@yorku.ca

doi:10.1158/1541-7786.MCR-05-0174

Introduction

Ovarian carcinoma is the most fatal gynecologic malignancy and is the fourth leading cause of cancer death in women (1-3). The epithelial ovarian cancer (EOC), arisen from the ovarian surface epithelium (OSE), constitutes ~90% of cases of ovarian cancer (4). The transforming growth factor-β (TGF-β) superfamily has been implicated in many developmental, physiologic, and pathologic processes, including tumorigenesis (5-8). Several members of the TGF-β superfamily, including TGF-β, activin/inhibin, and bone morphogenetic protein-4, have been shown to regulate proliferation and apoptosis in OSE and EOC cells (7, 9-12). Recently, we showed that Nodal, which is known as an important regulator of embryogenesis (13, 14), inhibits proliferation and induces apoptosis in several EOC cell lines (15), suggesting a role for Nodal in ovarian tumorigenesis.

Members of TGF-β superfamily exert their functions by interacting with type I and II serine/threonine kinase receptors (5-8). They bind to the type II receptors and then combine with the type I receptors to form a complex. The type I receptors are subsequently phosphorylated by the type II receptors and in turn activate intracellular substrates, such as Smad proteins (5-8, 16). Receptor-regulated Smads are activated by type I receptors through phosphorylation, form complex with Smad4, and translocate into the nucleus to regulate gene transcription (5-8, 16). Currently, seven type I receptors, called activin receptor-like kinase (ALK) 1-7, have been characterized in mammals (6, 7). ALK4, ALK5, and ALK7 form a subgroup of the type I receptors that activate Smad2 and Smad3 (7, 17).

ALK7 was first discovered in the rat as an orphan receptor (18, 19). The human ALK-7 cDNA was subsequently cloned (20, 21). Our laboratory has also identified additional isoforms of ALK7, including two soluble isoforms and a transmembrane isoform, which is truncated by 50 amino acids in the NH_2 terminus, generated by alternative splicing (21). Thus far, three ligands have been identified for ALK7: Nodal (22) and activin AB and activin B (23). Nodal was found to signal through activin receptor type IIB (ActRIIB) and ALK4 or ALK7 during embryonic development (22). Recently, ALK7 was also reported to form a complex with active receptor type IIA to transmit activin B and activin AB signals in pancreatic cells (23).

Several studies have suggested a role for ALK7 in regulating various cellular functions. Activation of ALK7 has been

reported to inhibit cell proliferation and induce morphologic differentiation in a rat pheochromocytoma cell line, PC12 (24). Overexpression of constitutively active ALK7 (ALK7-ca) induced apoptosis in rat and human hepatoma cell lines (25). Our laboratory has shown that the overexpression of Nodal or ALK7-ca decreased cell proliferation and increased apoptosis in human trophoblast (26) and EOC (15) cell lines. The effect of Nodal was blocked by dominant-negative ALK7, indicating that Nodal acts through ALK7 to regulate cell proliferation and apoptosis (15, 26).

In mammalian cells, apoptosis is mediated by the death receptor and the mitochondrial pathways (27, 28). The death receptor pathway mainly activates caspase-8, which in turn activates downstream effector caspases, including caspase-3, caspase-6, and caspase-7. In the mitochondrial pathway, cytochrome *c* from the mitochondria binds and activates apoptosis protease activating factor-1, which in turn activates caspase-9 (27, 28). Similar to caspase-8, caspase-9 also activates the same effector caspases. Bcl-2 and Bcl-X_L are antiapoptotic factors that inhibit apoptosis by associating with proapoptotic factors, Bak and Bax, at the mitochondrial membrane to prevent the release of cytochrome *c* (27, 28). Xiap is a key member of the inhibitor of apoptosis protein family, which blocks apoptosis by inhibiting the activity of caspase-9, caspase-3, and caspase-7 (29). ALK7 has been reported to trigger cytochrome *c* release in hepatoma cells (25). In ovarian cancer cells, we have shown that ALK7 activation elevated caspase-9 activity and down-regulated Xiap expression (15). These findings suggest that ALK7 induces apoptosis through the mitochondrial pathway. However, the precise molecular and cellular mechanism by which ALK7 induces apoptosis remains largely unknown.

The aim of this study was to explore the cellular and molecular mechanisms underlying ALK7-induced apoptosis in normal and malignant ovarian epithelial cells. We identified several molecules specifically the Bcl-2 family and Xiap that are important in mediating ALK7-induced apoptosis.

Results

Expression of ALK7 and Its Related Signaling Molecules in Ovarian Epithelial Cells

We have shown previously the mRNA expression of Nodal, ALK7, and their downstream mediators, Smads, in several EOC cell lines (15). To determine whether IOSE397 cells also express Nodal-ALK7 signaling molecules, reverse transcription-PCR (RT-PCR) was done. Using primers that span exons III and IV of the *ALK7* gene (15, 21), three DNA fragments corresponding to the expected sizes of three ALK7 transcripts, ALK7-1, ALK7-3, and ALK7-4, were detected in both IOSE397 and OV2008 cells (Fig. 1). The expression of ALK7-2 was also observed after RT-PCR using a sense primer that is specific for transcript 2 and an antisense primer common to all transcripts. Furthermore, RT-PCR with specific primers detected the expression of Nodal, ActRIIB, Smad2, Smad3, and Smad4 in both cell lines (Fig. 1).

Activation of ALK7 Induces Apoptosis in IOSE397 and OV2008 Cells

Infection of IOSE397 and OV2008 cells with various adenovirus constructs, Ad-GFP, wild-type ALK7 (Ad-ALK7-wt), or Ad-ALK7-ca, yielded ~95% efficiency as estimated by the green fluorescent protein (GFP) expression. Cells infected with Ad-GFP and Ad-ALK7-wt had a similar growth rate, whereas Ad-ALK7-ca significantly increased the number of dead cells when compared with Ad-GFP-infected and Ad-ALK7-wt-infected groups in both cell lines at all time points tested. On the other hand, Ad-ALK7-ca significantly decreased the number of live cells starting at 48 hours postinfection. All Ad-ALK7-ca-infected IOSE397 cells died at 72 hours postinfection, whereas some of the OV2008 cells stayed alive until 120 hours after infection (Fig. 2). When compared with the mock-infected control, Ad-GFP also caused some cell death (Fig. 2), suggesting that the adenoviral vector has some toxicity in these cells.

To determine if the cell death induced by Ad-ALK7-ca was due to apoptosis, several experiments were done. Using Hoechst staining technique, we observed that ALK7-ca induced

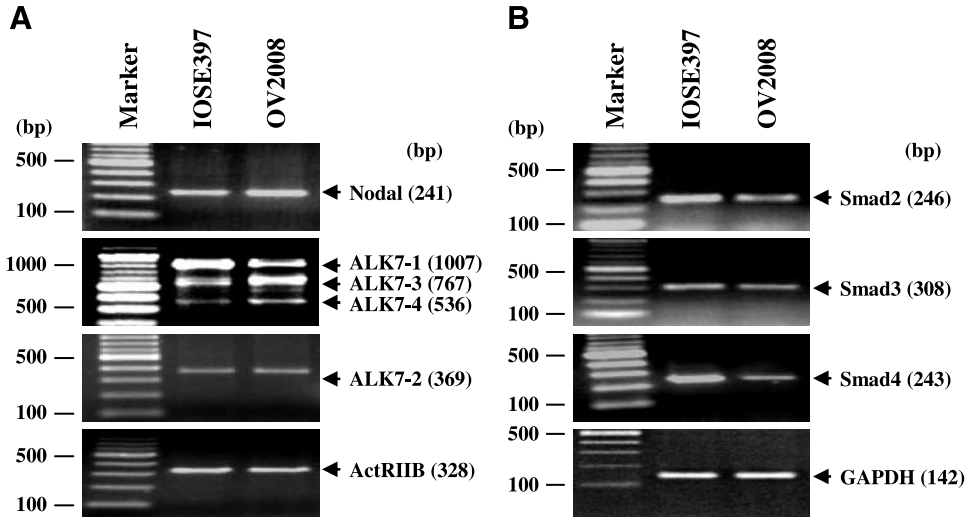

FIGURE 1. Expression of four ALK7 transcripts and mRNAs of Nodal, ActRIIB, Smad2, Smad3, and Smad4 in IOSE397 and OV2008 cells. Total RNA was extracted from both cell lines and subjected to RT-PCR using specific primers. Glyceraldehyde-3-phosphate dehydrogenase (*GAPDH*) was used as an internal control. Representative experiment.

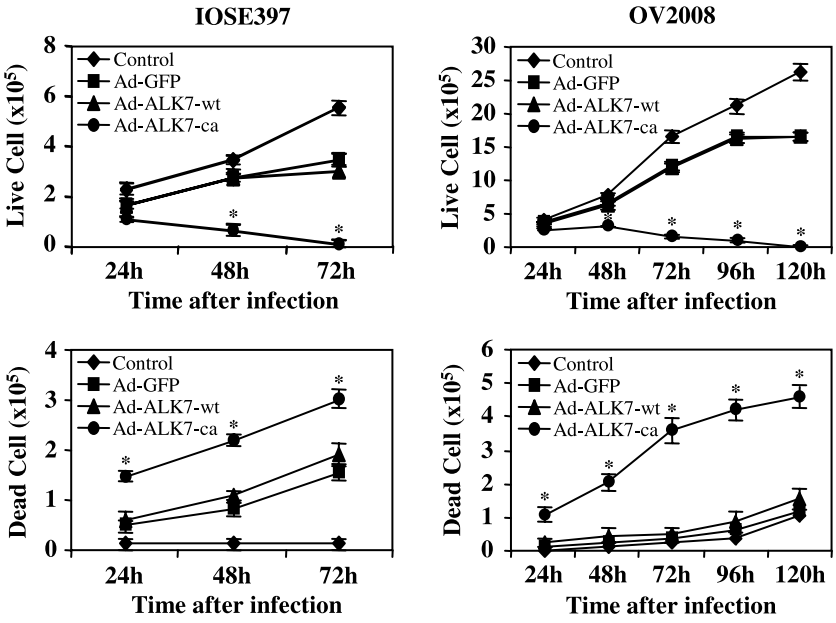

FIGURE 2. Effect of ALK7-ca on ovarian epithelial cell growth and viability. IOSE397 and OV2008 cells were seeded into 6-cm dishes and infected with Ad-GFP, Ad-ALK7-wt, or Ad-ALK7-ca for 4 hours. The number of live and dead cells was determined by trypan blue exclusion at different time points after infection. Cells without infection were used as an internal control. Points, mean (n = 5 dishes); bars, SE. *, $P < 0.05$ versus noninfected control, Ad-GFP, and Ad-ALK7-wt at the same time point. The experiment was repeated twice with similar results.

typical apoptotic nuclear morphology, such as nuclear shrinkage, condensation, and fragmentation, in IOSE397 and OV2008 cells (Fig. 3A). MitoShift assays and Western blot analyses were done to determine if there is a disruption of mitochondrial membrane potential and a release of cytochrome *c*. IOSE397 and OV2008 cells were infected with Ad-GFP, Ad-ALK7-wt, or Ad-ALK7-ca, and at 24 hours (IOSE397) or 48 hours (OV2008) after infection, cells were subjected to MitoShift assays or protein extraction. In control cells, the dye was located in the mitochondria and appeared as a punctate, perinuclear, red staining of fluorescence (Fig. 3B). In cells infected with Ad-ALK7-ca, the dye shifted out of the mitochondria to the cytoplasm, where it produced a diffuse fluorescence, indicating the disruption of the mitochondrial membrane potential (Fig. 3B). Western blots of cytosolic and mitochondrial proteins probed by anti–cytochrome *c* antibody revealed that there was an increase in cytochrome *c* in the cytosolic fraction after Ad-ALK-ca infection (Fig. 3C). Finally, the activation of caspase-9 and caspase-3 was determined by Western blot analyses. In both cell lines, the level of cleaved fragments of caspase-3 and caspase-9 was increased at 24 hours after infection with Ad-ALK7-ca, whereas the procaspase-3 and procaspase-9 levels were slightly decreased (Fig. 3D). To confirm the activation of caspases, the blots were reprobed with an antibody against poly(ADP-ribose) polymerase (PARP), a substrate of caspase-3, and an increase in PARP cleavage was observed in Ad-ALK7-ca-infected cells (Fig. 3D).

Effects of Ad-ALK7-ca on Bcl-2 Family and Xiap Expression

Because the Bcl-2 family plays major roles in regulating apoptosis by controlling the release of cytochrome *c* from mitochondria and interfering with mitochondrial membrane functionality, we next investigated whether ALK7 alters the expression of Bcl-2, Bcl-X_L, and Bax at mRNA and protein levels. Infection with Ad-ALK7-ca resulted in a decrease in Bcl-X_L mRNA levels at 24 hours after infection in both cell lines (Fig. 4A). Bcl-X_L protein contents were also decreased by Ad-ALK7-ca in IOSE397 and OV2008 cells (Fig. 4A). Similarly, Bcl-2 expression at mRNA and protein levels in both cell lines was also reduced by Ad-ALK7-ca (Fig. 4B) at 24 hours postinfection. On the other hand, the expression of proapoptotic factor, Bax, was increased after Ad-ALK7-ca infection at both mRNA and protein levels (Fig. 4B). Ad-ALK7-ca significantly reduced the ratio of Bcl-2 to Bax (Fig. 4B). The basal expression level of antiapoptotic factors, Bcl-2 and Bcl-X_L, was higher in OV2008 cells than in IOSE397 cells, whereas the basal level of proapoptotic regulator Bax was higher in IOSE397 cells than in OV2008 cells (Fig. 4A and B). It has been reported that caspases can cleave Bcl-2 and Bcl-X_L (30, 31); therefore, a general caspase-3 inhibitor, Z-VAD-fmk, was used to determine whether the decrease in Bcl-2 and Bcl-X_L contents observed after Ad-ALK7-ca infection is affected by the activation caspases. As shown in Fig. 4C, the caspase inhibitor did not block the effect of Ad-ALK7-ca on Bcl-2 and Bcl-X_L expression, suggesting that the decrease in Bcl-2 and Bcl-X_L contents after Ad-ALK7-ca infection is not due to their cleavage by caspases. Both mRNA and protein levels of Xiap were also decreased by Ad-ALK7-ca in IOSE397 and OV2008 cells (Fig. 4C).

Bax Silencing Partially Blocks ALK7-Induced Apoptosis

To confirm the involvement of Bax in ALK7-induced apoptosis, we used small interfering RNA (siRNA) to silence Bax expression. IOSE397 cells were transiently transfected with either control-siRNA or Bax-siRNA and then infected with Ad-GFP or Ad-ALK7-ca. As shown in Fig. 5A, ALK7-ca increased Bax protein expression in mock-transfected cells and cells transfected with the control-siRNA. Bax-siRNA greatly reduced the expression level of Bax and no induction of Bax was observed after Ad-ALK7-ca infection. Ad-ALK7-ca activated caspase-3 in mock-transfected and

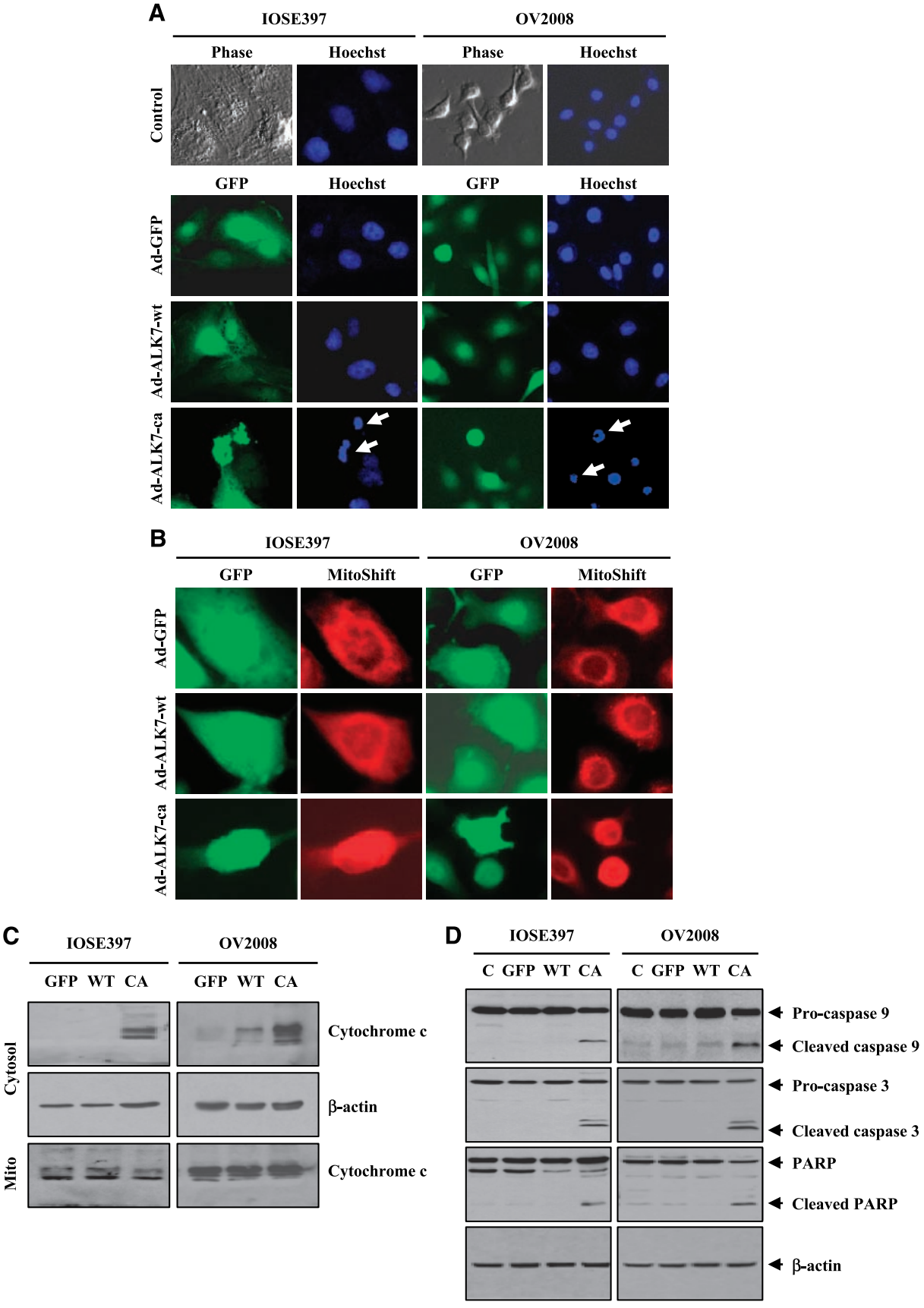

control-siRNA-transfected cells; however, the Ad-ALK7-ca-activated caspase-3 was reduced in Bax-siRNA-treated cells. On the other hand, silencing of the *Bax* gene did not alter the effect of Ad-ALK7-ca on Xiap expression (Fig. 5A). When apoptosis was quantified using a terminal deoxynucleotidyl transferase–mediated dUTP nick end labeling (TUNEL) assay, we found that the Ad-ALK7-ca-induced apoptosis was significantly reduced, but not completely blocked, in cells pretreated with Bax-siRNA (Fig. 5B and C).

Regulation of Bax and Xiap by ALK7 Is Smad Dependent

To further define the biochemical pathways underlying ALK7-induced apoptosis, we sought to determine whether ALK7 induces apoptosis by activating the Smad signaling cascade to up-regulate Bax and down-regulate Xiap. Western blot analysis was first done to measure total and phosphorylated Smad2 and Smad3 levels. In both IOSE397 and OV2008 cells, Ad-ALK7-ca increased Smad2 and Smad3 phosphorylation without altering total Smad2 and Smad3 levels (Fig. 6A). A noticeable difference between the two cell lines was that the basal level of phosphorylated Smad2 was higher in IOSE397 cells than in OV2008 cells (Fig. 6A). Subsequently, we tested the translocation of Smad2 into the nucleus following Ad-ALK7-ca infection or incubation with recombinant mouse Nodal. Smad2 was mainly located in cytoplasm of the Ad-GFP-infected cells, but it was predominantly detected in the nucleus of Ad-ALK7-ca-infected cells (Fig. 6B). Similarly, Smad2 was mainly distributed in cytoplasm before the treatment of the recombinant mouse Nodal. After 5 minutes of Nodal treatment, Smad2 was translocated from the cytoplasm into the nucleus (Fig. 6C). On Nodal treatment for 24 hours, the level of Bax protein content was increased, whereas Bcl-X_L was decreased (Fig. 6D). Finally, the role of Smads in ALK7-ca-regulated and Nodal-regulated gene expression was examined using a dominant-negative strategy. IOSE397 cells were transiently transfected with dominant-negative Smad2 (DN-Smad2) or Smad3 (DN-Smad3) for 5 hours and recovered overnight before infection with the adenoviral constructs. Again, ALK7-ca increased the expression of Bax and activated caspase-3 and decreased the expression of Xiap. However, these effects were abolished by cotransfection of DN-Smad2 or DN-Smad3 (Fig. 7A). Similarly, transient transfection of Nodal also increased Bax expression and caspase-3 activation but decreased Xiap expression. In the presence of DN-Smad4, these effects of Nodal were diminished (Fig. 7B). The effectiveness of DN-Smad constructs was confirmed by examining Smad4 localization after DN-Smad2 or DN-Smad3 transfection. As shown in Fig. 7C, Nodal induces Smad4 translocation from the cytoplasm to the nucleus and the effect of Nodal was blocked by either DN-Smad2 or DN-Smad3.

Discussion

Previously, we have reported that activation of the Nodal-ALK7 pathway leads to the induction of apoptosis and activation of caspase-9 and caspase-3 in ovarian cancer cell lines (15). However, how Nodal-ALK7 signaling triggers the activation of these caspase molecules was largely unclear. In the present study, we investigated the mechanisms underlying ALK7-induced apoptosis. Specifically, we have identified Bcl-2 family and Xiap as two Smad2/3-dependent pathways in mediating the proapoptotic action of Nodal-ALK7.

We have characterized previously four human ALK7 transcripts derived from alternative splicing of the *ALK7* gene (21). In the present study, we found that four transcripts of ALK7, along with its ligand, Nodal, the type II receptor partner, and their downstream signaling molecules, Smads, were also expressed in an immortalized human OSE cell line, IOSE397. This suggests that the Nodal-ALK7-Smad signaling pathway plays a role in IOSE cells. This notion was further supported by findings that Nodal and/or ALK7-ca activated Smad2, Smad3, Bax, and caspase-3 and inhibited Xiap expression and that ALK7-ca potently induced apoptosis in IOSE397 cells.

Using the adenovirus delivery method, we showed that activation of ALK7 potently induced cell death. Previously, we found a 30% decrease in cell numbers after 72 hours of transient transfection with Nodal or ALK7-ca in EOC cell lines (15). In this study, all IOSE397 cells died and there was >70% decrease in OV2008 cells at 72 hours after infection with Ad-ALK7-ca. The different potency of ALK7-ca observed in these studies is most likely due to the use of different gene delivery methods. The adenovirus method used in this study yielded a 95% infection rate, whereas transient transfection of plasmid DNA used in our previous study had an efficiency of ~50%. Interestingly, we found that although ALK7-ca inhibited growth and induced cell death in both IOSE397 and OV2008 cells, IOSE397 cells were more sensitive to ALK7-ca than OV2008 cells as, following Ad-ALK7-ca infection, IOSE397 cells only survived for 3 days, whereas OV2008 cells lasted for 5 days. Several differences between the nontumorigenic IOSE397 and the cancer cell line OV2008 were observed: (*a*) basal phosphorylated Smad2 levels were higher in IOSE cells than in OV2008 cells; (*b*) OV2008 had higher levels of antiapoptotic

FIGURE 3. Induction of apoptosis by ALK7 in IOSE397 and OV2008 cells. Cells were infected with Ad-GFP, Ad-ALK7-wt, or Ad-ALK7-ca. Uninfected cells were used as an internal control. **A.** Hoechst staining. White arrows, apoptotic nuclei. Photographs were taken after 48 hours (*IOSE*) and 72 hours (*OV2008*) postinfection by fluorescence microscopy. Original magnification, ×200. **B.** Assessment of mitochondrial membrane potential. MitoShift assay was done at 24 hours (*IOSE397*) and 48 hours (*OV2008*) postinfection. In cells infected with Ad-GFP or Ad-ALK7-wt, the MitoShift dye was located in the mitochondria and appeared as a punctate, perinuclear, red staining of fluorescence. In cells infected with Ad-ALK7-ca, the dye shifted out of the mitochondria to the cytoplasm, producing a diffuse fluorescence. Original magnification, ×300. **C.** Detection of cytochrome *c* by Western blot. IOSE397 and OV2008 cells were infected with Ad-GFP (*GFP*), Ad-ALK7-wt (*WT*), or Ad-ALK7-ca (*CA*) for 4 hours. Cytosolic and mitochondrial proteins were separated and cytochrome *c* was detected. **D.** Activation of caspase-3 and caspase-9 and cleavage of poly(ADP-ribose) polymerase (PARP). Total protein was extracted at 24 hours after infection, subjected to SDS-PAGE, and Western blotted using caspase-3, caspase-9, and PARP antibodies. β-Actin was used as a loading control. Representative experiment.

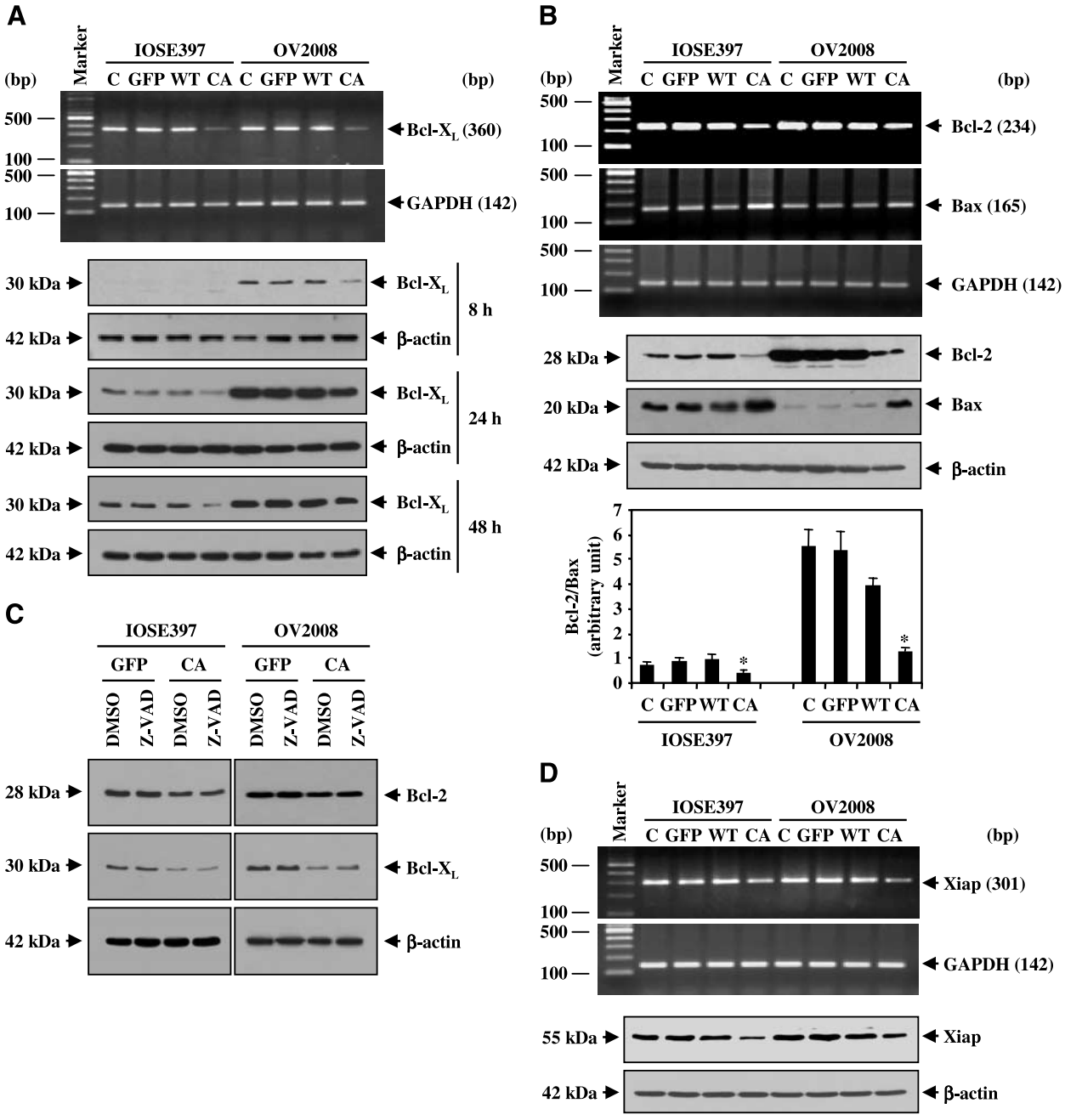

FIGURE 4. Regulation of Bcl-2 family and Xiap expression by ALK7. IOSE397 and OV2008 cells were infected without (*C*; control) or with Ad-GFP, Ad-ALK7-wt, or Ad-ALK7-ca for 4 hours and recovered for a period. **A.** Expression of Bcl-X_L mRNA (24 hours postinfection) as detected by RT-PCR and protein (8-48 hours postinfection) as measured by Western blotting. ALK7-ca decreased Bcl-X_L mRNA and protein levels. **B.** ALK7-ca decreased Bcl-2 and increased Bax mRNA (*top*) and protein (*middle*) expression at 24 hours after infection with Ad-ALK7-ca. Bottom, ratio of Bcl-2/Bax. Columns, mean of four experiments; bars, SE. *, $P < 0.05$ versus other groups. **C.** Effect of a caspase inhibitor on ALK7-mediated Bcl-2 and Bcl-X_L expression. Cells were preincubated with Z-VAD-fmk or DMSO for 2 hours followed by infection with either Ad-GFP or Ad-ALK7-ca for 4 hours. ALK7-ca decreased the expression of Bcl-2 and Bcl-X_L expression after 16 hours and the effect of ALK7 on Bcl-2 and Bcl-X_L was not influenced by pretreatment with the caspase inhibitor. **D.** Expression of Xiap mRNA and protein as determined by RT-PCR and Western blotting, respectively. Both RNA and protein samples were collected at 24 hours after infection and Xiap levels were found to be suppressed by ALK7-ca. Glyceraldehyde-3-phosphate dehydrogenase and β-actin were used as controls for RT-PCR and Western blot analysis, respectively.

factors, such as Bcl-2 and Bcl-X_L, than IOSE397 cells; and (*c*) the level of proapoptotic factor, Bax, was higher in IOSE cells than in OV2008 cells. Because we have shown that Smad2, Bax, Bcl-2, and Bcl-X_L are all downstream signaling components of the ALK7 pathway, it is possible that the differential expression of these proteins in IOSE397 and OV2008 cells contributes to their different susceptibility to ALK7-induced cell death.

In mammals, two basic apoptotic pathways, the cytokine-mediated mitochondrial pathway and the death receptor pathway, have been defined (27, 28, 32, 33). Previous studies have shown that activation of ALK7 leads to cytochrome *c* release in hepatoma cells (25) and caspase-9 activation in ovarian cancer cells (15). In this study, we further examined the involvement of the mitochondrial pathway in ALK7-mediated apoptosis. Ad-ALK7-ca induced an up-regulation of Bax and a down-regulation Bcl-2 and Bcl-X_L expression and caused a disruption of the mitochondrial membrane potential as well as an increase in cytochrome *c* content in the cytosol. It is well documented that Bax translocates from cytosol to the outer membrane of mitochondria and regulates mitochondrial membrane permeability, allowing the passage of cytochrome *c* through the membrane (33). Bcl-2, on the other hand, inhibits apoptosis by preventing the release of cytochrome *c* via heterodimerization with Bax (34, 35). It is possible that, as the result of a decreased Bcl-2/Bax ratio following ALK7 activation, mitochondrial membrane potential is disrupted and this triggers the release of cytochrome *c*, leading to caspase-9 and caspase-3 activation and finally apoptosis. The importance of Bax in ALK7-induced apoptosis was further confirmed using the siRNA-mediated gene silencing technique. When Bax was knocked down, the effect of ALK7 on caspase-3 activation and apoptosis was significantly reduced but not completely blocked. This finding supports a role for Bax in ALK7-regulated apoptosis but also suggests that other molecules, independent of the Bax pathway, are also important for ALK7-induced apoptosis. Given that Ad-ALK7-ca also suppressed Xiap and Bcl-X_L expression in IOSE397 and OV2008 cells, it is likely that they also mediate the proapoptotic action of ALK7 in these cells.

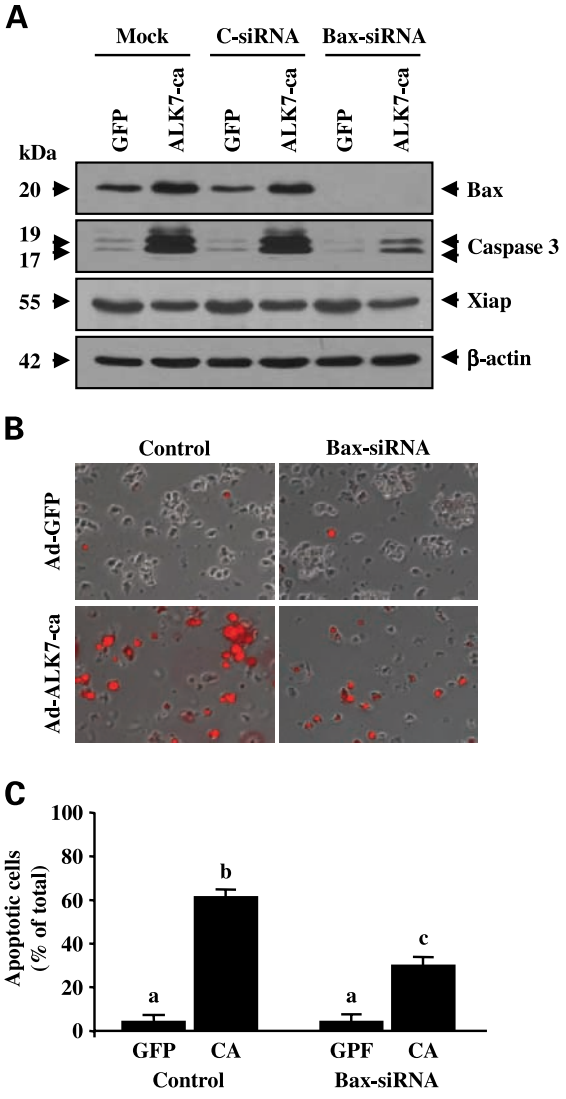

FIGURE 5. Effect of Bax-siRNA on the apoptotic action of ALK7 in IOSE397 cells. **A.** Detection of the expression of Bax, Xiap, and active caspase-3 by Western Blot. Cells were transiently transfected without (*mock*) or with control-siRNA (*C-siRNA*) or Bax-siRNA before the infection of Ad-GFP or Ad-ALK7-ca. Protein samples were extracted at 24 hours after infection and subjected to Western blot analyses with specific antibodies for Bax, Xiap, and active caspase-3. β-Actin was used as the loading control. Representative experiment. **B.** Detection of apoptotic cells by TUNEL assay. Total cells and apoptotic cells were photographed by phase-contrast microscopy and fluorescent microscopy, respectively. Two images were then merged and apoptotic cells appear red. Original magnification, ×100. **C.** Quantification of apoptotic cells. Total cell number and TUNEL-positive cell number were counted. Columns, mean of six randomly selected fields; bars, SE. Different letters denote statistical significance ($P < 0.05$). The experiment has been repeated and similar results were obtained.

Xiap inhibits apoptosis via inhibition of caspase-3, caspase-7, and caspase-9 activation (29) and is an important cell survival factor in human ovarian cancer cell lines (36). Overexpression of Xiap significantly prevented OV2008 cell apoptosis (36). Consistent with our previous studies in A2780 cells (15), we now found that ALK7-ca inhibited Xiap expression at both mRNA and protein levels in IOSE397 and OV2008 cells. In addition, we have also shown that down-regulation of Xiap expression by Nodal and ALK7-ca was reversed by DN-Smad2, DN-Smad3, or DN-Smad4, indicating that the Smad2/3 pathway is involved in Nodal/ALK7-regulated Xiap expression. Although TGF-β has been reported to inhibit Xiap expression in human hepatoma cell line HuH-7 (37) and in rat endometrial stromal decidual cells (38), to our knowledge, this is the first demonstration that Smads are involved in the regulation of Xiap expression. Because Smads are known to regulate gene transcription, it is likely that the decrease in Xiap mRNA and protein levels following ALK7 activation is due at least in part to the inhibition of Xiap gene transcription. Previous studies have shown that TGF-β1 stimulated ARTS, a protein that induces apoptosis by binding directly to Xiap and promoting its degradation (39). In addition, Xiap has also been shown to interact directly with type I TGF-β receptors, such as ALK1 (40), ALK4, ALK5, and, to a less extent, ALK2 and ALK3 (40), and functions as a Smad cofactor to activate Smad-dependent signaling (41, 42). It remains to be determined whether the Nodal-ALK7 pathway also acts through ARTS to decrease Xiap content in the ovarian cells and Xiap can interact directly with ALK7.

ALK7 has been shown to use a similar Smad2/3 signaling pathway as ALK4 and ALK5, which mediate signaling by activin and TGF-β, respectively (7, 17). In this study, we found that Nodal and ALK7-ca induced translocation of Smad2 into the nucleus and activated Smad2 and Smad3. The

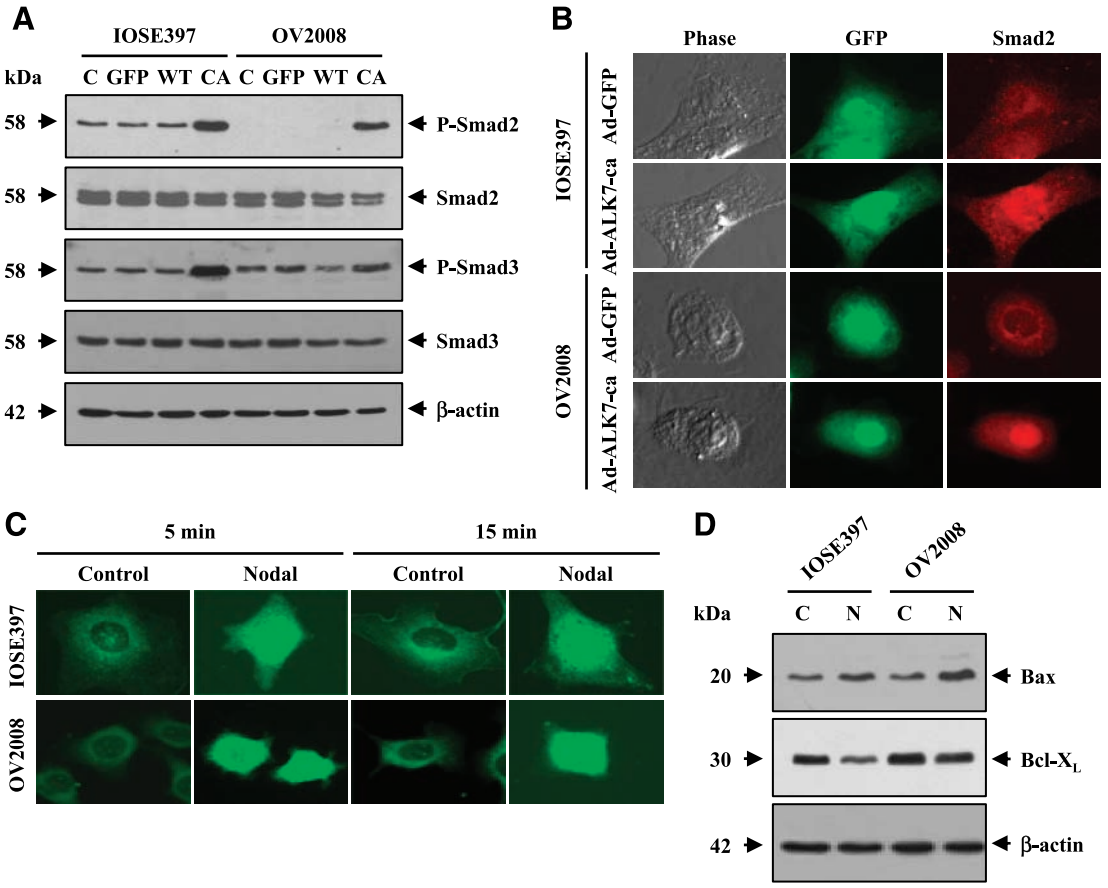

FIGURE 6. Activation of Smad2/3 by Nodal and ALK7. **A.** Cells were infected without or with Ad-GFP, Ad-ALK7-wt, or Ad-ALK7-ca for 4 hours and recovered for 24 hours. Total protein was subjected to SDS-PAGE. Phosphorylated Smad2 (*P-Smad2*), total Smad2, phosphorylated Smad3 (*P-Smad3*), and total Smad3 were detected using specific antibodies. β-Actin was used as the loading control. Representative experiment. **B.** Detection of the cellular localization of Smad2 in Ad-GFP-infected and Ad-ALK7-ca-infected cells. Photographs were taken by phase-contrast microscopy and fluorescence microscopy at 4 hours after infection. **C.** Detection of Smad2 translocation in Nodal-treated cells. Cells were incubated with recombinant Nodal (500 ng/mL) for 5 or 15 minutes and cellular localization of Smad2 was examined by fluorescence microscopy using specific antibody against Smad2. Original magnification, ×300. **D.** Detection of Bax and Bcl-X_L expression. IOSE397 and OV2008 cells were treated with Nodal (500 ng/mL) for 24 hours and protein was extracted and subjected to Western blot. Bax and Bcl-X_L were detected using specific antibodies. β-Actin was used as the loading control. C, control; N, Nodal.

involvement of Smad2/3 pathway in ALK7-induced apoptosis was further supported by the finding that DN-Smad2, DN-Smad3, and DN-Smad4 blocked caspase-3 activation by ALK7-ca or Nodal. This finding is consistent with a recent report that knockdown of Smad3 attenuated ALK7-induced apoptosis in hepatoma cells (25). Although acting through a common Smad2/3 pathway, Nodal, activin, and TGF-β seem to have somewhat different functions in ovarian cells. TGF-β has antiproliferative and proapoptotic effects in early neoplastic and tumorigenic OSE cell lines (9) and EOC cells from patients (10, 11). However, some ovarian carcinoma cells have become resistant to growth inhibitory effect of TGF-β (43). In contrast, activin has been reported to promote cell proliferation in several EOC cell lines, such as CaOV4, SKOV3, and OVCAR3 (9, 44). However, activin had no effect on normal OSE cells (9) but inhibited cell proliferation in early neoplastic and tumorigenic OSE cells (45). In IOSE cell lines, Choi et al. (9) observed a decrease in Bcl-2 and no change in Bax protein levels after TGF-β treatment and no effect of activin on either Bcl-2 or Bax expression. In our studies using IOSE397 and several EOC cell lines, including OV2008, C13*, A2780-s, and A2780-cp (this study and ref. 15), we have consistently observed an inhibition of cell growth and induction of apoptosis by the Nodal-ALK7 pathway. These findings suggest that activin, Nodal, and TGF-β may have distinct targets in the OSE and EOC cells. This further supports the complex nature of the Smad pathway. Interestingly, in addition of the Smad pathway, the mitogen-activated protein kinase pathways also mediate the apoptotic action of ALK7 in hepatoma cells (25). Similarly, p38 and c-Jun NH_2-terminal kinase pathways have been shown to be involved in TGF-β-induced apoptosis (46). Whether these pathways also play a role in ALK7-mediated apoptosis in ovarian cells will be examined in the future.

Taken together, we have shown that normal and malignant ovarian epithelial cell lines, IOSE397 and OV2008, expressed the signaling molecules of the Nodal-ALK7 pathway, including

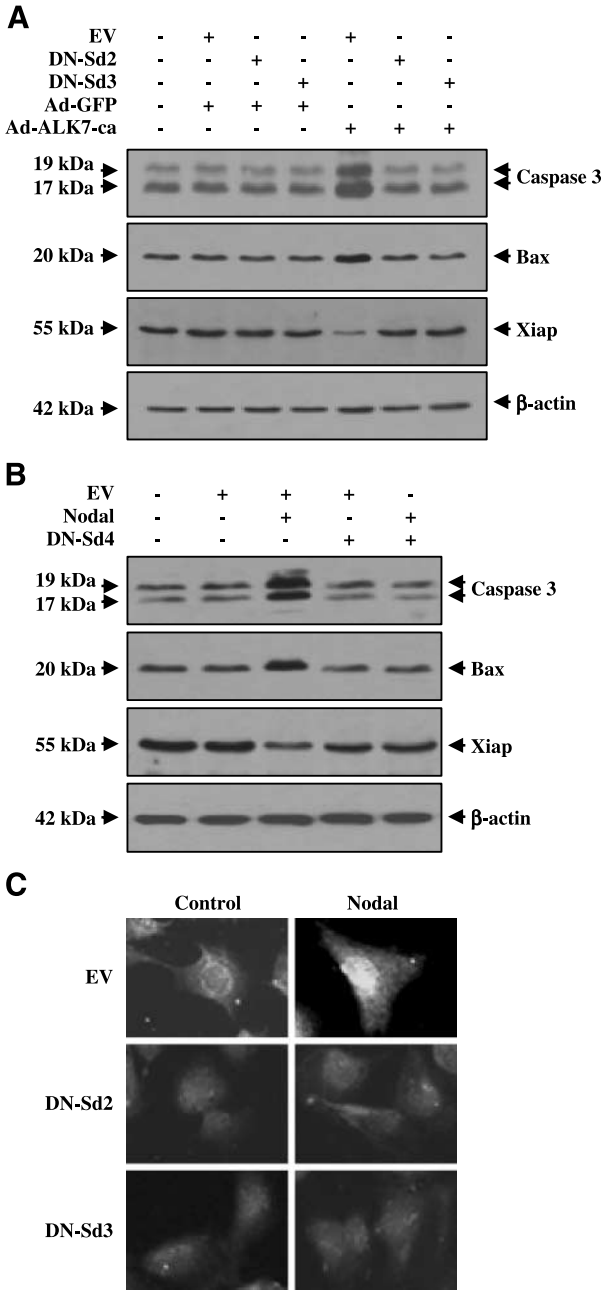

FIGURE 7. Involvement of Smad2/3 in Nodal and ALK7 actions. **A.** IOSE397 cells were transiently transfected with empty vector (*EV*), DN-Smad2 (*DN-Sd2*), or DN-Smad3 (*DN-Sd3*) followed by infection with Ad-GFP or Ad-ALK7-ca. Proteins were extracted at 24 hours after infection and subjected to Western blotting using antibodies specific for cleaved caspase-3, Bax, and Xiap. DN-Smad2 and DN-Smad3 blocked the effect of ALK7-ca on Bax and Xiap expression and caspase-3 activation. **B.** IOSE397 cells were cotransfected with pcDNA3.1-Nodal-V5 (*Nodal*), and either the control vector (*EV*) or DN-Smad4 (*DN-Sd4*). Proteins were prepared at 24 hours after transfection and analyzed by Western blotting. Nodal increased the activation of caspase-3 and Bax but decreased the expression of Xiap and this effect was blocked by dominant-negation Smad4. β-Actin was used as the loading control. Representative experiment. **C.** Immunofluorescence staining of Smad4. IOSE397 cells were transfected with empty vector, DN-Smad2, or DN-Smad3 followed by recombinant Nodal (500 ng/mL) treatment. Cellular localization of Smad4 was examined by fluorescence microscopy using a specific antibody against Smad4. DN-Smad2 and DN-Smad3 both blocked Nodal-induced Smad4 translocation to the nucleus. Original magnification, ×300.

the ligand, receptors, and Smads. ALK7-ca-induced ovarian epithelial cell apoptosis was due at least in part to the disruption of mitochondrial membrane potential through the regulation of Bcl-2 family, such as Bax, Bcl-2, and Bcl-X_L. Silencing of *Bax* gene partially blocked the action of ALK7-ca, indicating the involvement of multiple pathways in ALK7-induced apoptosis. In addition, Xiap expression was down-regulated by ALK7 through a Smad2/3-dependent pathway. Based on these findings and the known function of Bax and Xiap, we proposed that Bax/Bcl-2 and Xiap are in part involved in Nodal/ALK7-induced apoptosis (Fig. 8). Nodal acts through ActRIIB and ALK7 to induce Smad2/3 activation, which in turn regulates the expression of Bax, Bcl-2, and Xiap. The decrease in Bcl-2/Bax ratio results in the release of cytochrome *c* and subsequent activation of caspase-3. The decrease in Xiap expression also leads to caspase-3 activation and apoptosis. Future studies are necessary to verify this and to identify additional pathways mediating the apoptotic action of Nodal and ALK7.

Materials and Methods

Cell Lines and Cell Culture

A human immortalized OSE cell line, IOSE397, was developed by transfecting normal OSE cells with SV40 large T antigen, similar to the establishment of IOSE29 cell line (9). The cell line exhibits no tumorigenic behavior. IOSE397 cells were cultured in M199 and MCDB105 (1:1; both from Sigma, Oakville, Ontario, Canada) supplemented with 5% fetal bovine serum (HyClone, Logan, UT) and 50 μg/mL gentamicin (Sigma). OV2008 cells were cultured as described previously (15).

RNA Extraction and RT-PCR

Total RNA was extracted from cells using Trizol reagent (Invitrogen, Burlington, Ontario, Canada) and reverse transcribed as described previously (15). Primers of Nodal, ALK7, and its isoforms, ActRIIB, Smad2, Smad3, Smad4, Xiap, and glyceraldehyde-3-phosphate dehydrogenase, have been reported (15). Primers of Bcl-2 family are sense 5′-GGATTGTGGCCTTCTTTGAG-3′ and antisense 5′-CCAAACTGAGCAGAGTCTTC-3′ for Bcl-2, sense 5′-AAGGGACAGAATCGGAGATG-3′ and antisense 5′-TCTCCTTGTCTACGCTTTCC-3′ for Bcl-X_L, and sense 5′-AGACAGGGGCCCTTTTGCTTC-3′ and antisense 5′-TGCAGCTCCATGTTACTGTCC-3′ for Bax. PCR was done for 18 to 40 cycles, with annealing temperatures from 55°C to 60°C depending on the target genes.

Generation of Expression Constructs

Human Nodal expression plasmid, pcDNA3.1-Nodal-V5-His, was subcloned from pcDNA4-Nodal-myc (15). DN-Smad4 was kindly provided by Dr. Rik Derynck (University of California at San Francisco, San Francisco, CA) and subcloned into pcDNA3.1 (Invitrogen). Adenoviral construct with GFP carrying a ALK7-ca (Ad-ALK7-ca) or ALK7-wt (Ad-ALK7-wt) was generated using AdEasy System (47). Recombinants were selected by kanamycin resistance and further confirmed by multiple restriction enzyme analyses.

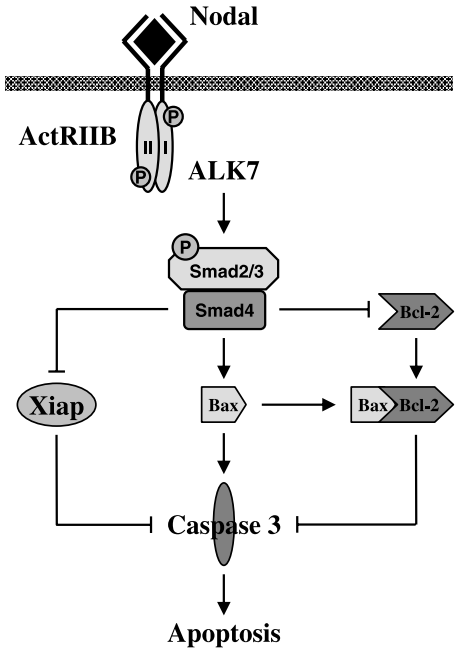

FIGURE 8. Proposed mechanisms underlying the apoptotic action of Nodal/ALK7 in ovarian epithelial cells. Nodal binds to a receptor complex consisting of ActRIIB/ALK7 and activates Smad2/3. The activated Smads in turn suppress Xiap and Bcl-2 expression but increase Bax expression. The decrease in Bcl-2/Bax ratio allows the release of cytochrome *c*, leading to caspase-3 activation. The decrease in Xiap expression also enhances caspase-3 activation. Thus, Xiap and Bax/Bcl-2 are two Smad-dependent pathways, which mediate at least in part the apoptotic action of Nodal/ALK7 in ovarian epithelial cells.

Transient Transfection and Adenoviral Infection

IOSE397 and OV2008 cells were seeded into six-well plates at a density of 2×10^5 per dish and cultured for 24 hours before transfection or infection. Transient transfection was done as described previously (15). For adenoviral infection, IOSE397 and OV2008 cells were incubated without (control) or with Ad-GFP, Ad-ALK7-wt, or Ad-ALK7-ca for 4 hours and then switched to a complete medium for additional 24 to 120 hours. The adenoviral construct was used at a concentration of 3×10^9 plaque-forming units/mL ($\sim$10 multiplicities of infection). In experiments involving the use of a caspase inhibitor, cells were first treated with 50 μmol/L of a general caspase inhibitor, Z-VAD-fmk (BD Biosciences, Mississauga, Ontario, Canada), for 2 hours before adenoviral infection. DMSO was used as a vehicle control. Cells were then infected with Ad-GFP or Ad-ALK7-ca for 4 hours and recovered for 16 hours.

Determination of Cell Growth and Viability

Cell survival/death was assessed by 0.2% trypan blue staining (Invitrogen). At 1 to 5 days following infection with various adenoviral constructs, floating cells were collected from culture medium and attached cells were trypsinized. The two cell populations were then combined and cell number was determined by manual cell counting using hemocytometry.

Hoechst Staining of Nuclei

Hoechst-33258 (bisbenzimide, Sigma) staining was carried out as reported previously (15) with slight modifications. Briefly, IOSE397 and OV2008 cells were plated into 6-cm dishes and infected with various adenoviral constructs for 4 hours and then cultured in complete medium for 48 and 72 hours, respectively. Cells were fixed *in situ* with 10% phosphate-buffered formalin for 5 minutes and stained with Hoechst at 37°C for 30 minutes. Typical apoptotic nuclear morphology (nuclear shrinkage, condensation, and fragmentation) was viewed under a fluorescent microscope (TE2000, Nikon Canada, Inc., Mississauga, Ontario, Canada). Photographs were taken using a Qimaging Digital Camera (Nikon) with SimplePCI Imaging Software (Compix Inc., Township, PA).

MitoShift Assay

The mitochondrial membrane potential was determined using a MitoShift kit (Trevigen, Inc., Gaithersburg, MD) according to the manufacturer's instructions. Briefly, IOSE397 and OV2008 cells were infected with adenoviral constructs as described above and recovered for 24 and 48 hours, respectively. After washing with the reaction buffer, cells were incubated with a MitoShift dye (tetramethylrhodamine methylester) for 60 minutes at room temperature followed by two washes with the reaction buffer. Cells were then viewed under the fluorescence microscope and photographed.

Protein Extraction and Western Blot Analysis

Whole-cell lysates were prepared as described previously (15). Fractionation of cytosolic and mitochondrial proteins was prepared according to a previous report (35). Briefly, cells were trypsinized and collected by centrifugation. Following two washes with ice-cold PBS, the cell pellet was resuspended in 300 μL extraction buffer containing 20 mmol/L HEPES-KOH (pH 7.5), 10 mmol/L KCl, 1.5 mmol/L $MgCl_2$, 1 mmol/L EDTA, 1 mmol/L EGTA, 1 mmol/L DTT, 0.1 mmol/L phenylmethylsulfonyl fluoride, and 250 mmol/L sucrose. The cells were then homogenized with a Teflon homogenizer and centrifuged at $750 \times g$ for 10 minutes at 4°C. The supernatants were centrifuged at $10{,}000 \times g$ for 30 minutes at 4°C to pellet mitochondria. The collected supernatant was further centrifuged at $100{,}000 \times g$ for 1 hour to obtain cytosol. The mitochondrial pellets were washed twice and dissolved in the extraction buffer followed by sonication to disrupt the membrane of mitochondria. Protein samples subjected to SDS-PAGE and blotted as described previously (15). Rabbit anti-human cleaved caspase-3 and caspase-9, Xiap, and mouse anti-human β-actin antibodies have been described previously (15). Mouse anti-human caspase3 and caspase-9 and rabbit anti-human Bcl-2, Bcl-X_L, Bax, cytochrome *c*, PARP, Smad2, phosphorylated Smad2, and phosphorylated Smad3 were purchased from Cell Signaling Technology/New England Biolabs Ltd. (Pickering, Ontario, Canada) and used at 1:1,000 to 1:2,000 dilution. Rabbit anti-human Smad3 (1:500) was obtained from Zymed Laboratories, Inc. (South San Francisco, CA). Mouse anti-human Smad4 was purchased from Santa Cruz Biotechnology

(Santa Cruz, CA). Signals were detected using an Enhanced Chemiluminescence Plus kit (Amersham, Baie d'Urté, Québec, Canada) and visualized after exposure to a Bioflex Econo film (Clonex Corp., Markham, Ontario, Canada).

Bax-siRNA and TUNEL Assay

Cells were cultured into six-well plates at a density of 2×10^5 per well for 24 hours before transfection. After transient transfection with control-siRNA or Bax-siRNA (Cell Signaling Technology) at a final concentration of 100 nmol/L for 16 hours, cells were infected with Ad-GFP or Ad-ALK7-ca for 4 hours and then recovered in the complete medium for 24 hours. Mock transfection without siRNA was also done. The expression of target genes was determined by Western blot. Apoptotic cells were quantified by TUNEL assays (Roche Diagnostics, Laval, Quebec, Canada) following the manufacturer's suggested protocol. Briefly, cells were trypsinized and washed with PBS thrice before fixation in 4% paraformaldehyde. After permeabilization with 0.1% Triton X-100 in 0.1% sodium citrate for 4 minutes on ice, cells were incubated with the TUNEL assay reagent for 1 hour at 37°C. Cells were then washed with PBS twice and viewed under microscope. Total cell number was determined using phase-contrast microscopy, whereas apoptotic cells labeled by TUNEL were identified by fluorescence microscopy. Six randomly selected fields in each sample were scored for both total and TUNEL-positive cell numbers. At least 800 cells were counted in each preparation.

Immunofluorescence Staining

Immunofluorescence staining of Smad2 was done as described previously (48) with slight modifications. Briefly, IOSE397 and OV2008 cells were cultured for 24 hours before infection with adenoviral constructs or treatment with recombinant mouse Nodal (R&D Systems, Minneapolis, MN). After infection without (control) or with Ad-GFP or Ad-ALK7-ca for 4 hours and recovered for 4 hours or incubation without (control) or with 500 ng/mL Nodal for 5 or 15 minutes, cells were washed and fixed with 4% paraformaldehyde. Following permeabilization with 0.2% Triton X-100 and blocking with 1% bovine serum albumin, cells were incubated with rabbit anti-human Smad2 antibody (1:200 dilution; Cell Signaling Technology) at 4°C overnight. Control staining was carried out with nonimmune IgG used at the same concentration as the primary antibody. Subsequently, cells were incubated with fluorescent dye-conjugated goat anti-rabbit IgG (1:200 dilution; Molecular Probes, Burlington, Ontario, Canada) and signals were detected by the fluorescence microscopy. For immunostaining of Smad4, IOSE397 cells were cultured for 24 hours before transfection. After transient transfection with an empty vector, DN-Samd2, or DN-Smad3 for 5 hours and recovered for 4 hours, cells were treated with 500 ng/mL Nodal for 15 minutes. Cells were then fixed and stained.

Statistical Analysis

Data are mean ± SE of replicate samples in one experiment or replicate experiments as indicated in the figure legends. Student's t test was used for the comparison between two groups. Multiple group comparison was done by one-way ANOVA followed by a Tukey-Kramer multiple group comparisons test using the GraphPad InStat Software (GraphPad, Inc., San Diego, CA). Differences were considered significant at $P < 0.05$.

Acknowledgments

We thank Drs. Rik Derynck and Benjamin Tsang for providing the dominant-negative Smad plasmids and OV2008 cells, respectively.

References

1. Barnes MN, Grizzle WE, Grubbs CJ, Partridge EE. Paradigms for primary prevention of ovarian carcinoma. CA Cancer J Clin 2002;52:216–25.

2. Moss C, Kaye SB. Ovarian cancer: progress and continuing controversies in management. Eur J Cancer 2002;38:1701–7.

3. Jemal A, Murray T, Ward E, et al. Cancer statistics, 2005. CA Cancer J Clin 2005;55:10–30.

4. Parkin DM, Pisani P, Ferlay J. Global cancer statistics. CA Cancer J Clin 1999; 49:33–64.

5. Massagué J, Chen Y-G. Controlling TGF-β signaling. Genes Dev 2000; 6:627–44.

6. Chang H, Brown CW, Matzuk MM. Genetic analysis of the mammalian transforming growth factor-β superfamily. Endocr Rev 2002;23:787–823.

7. Peng C. The TGF-β superfamily and its roles in the human ovary and placenta. J Obstet Gynaecol Can 2003;25:834–44.

8. Narayan S, Thangasamy T, Balusu R. Transforming growth factor-β receptor signaling in cancer. Front Biosci 2005;10:1135–45.

9. Choi KC, Kang SK, Tai CJ, Auersperg N, Leung PC. The regulation of apoptosis by activin and transforming growth factor-β in early neoplastic and tumorigenic ovarian surface epithelium. J Clin Endocrinol Metab 2001; 86:2125–35.

10. Dunfield LD, Dwyer EJ, Nachtigal MW. TGF β-induced Smad signaling remains intact in primary human ovarian cancer cells. Endocrinology 2002; 143:1174–81.

11. Hurteau J, Rodriguez GC, Whitaker RS, et al. Transforming growth factor-β inhibits proliferation of human ovarian cancer cells obtained from ascites. Cancer 1994;74:93–9.

12. Shepherd TG, Nachtigal MW. Identification of a putative autocrine bone morphogenetic protein-signaling pathway in human ovarian surface epithelium and ovarian cancer cells. Endocrinology 2003;144:3306–14.

13. Brennan J, Norris DP, Robertson EJ. Nodal activity in the node governs left-right asymmetry. Genes Dev 2002;16:2339–44.

14. Nonaka S, Shiratori H, Saijoh Y, Hamada H. Determination of left-right patterning of the mouse embryo by artificial nodal flow. Nature 2002;418:96–9.

15. Xu G, Zhong Y, Munir S, Yang BB, Tsang BK, Peng C. Nodal induces apoptosis and inhibits proliferation in human epithelial ovarian cancer cells via activin receptor-like kinase 7. J Clin Endocrinol Metab 2004;89:5523–34.

16. Attisano L, Wrana JL. Signal transduction by the TGF-β superfamily. Science 2002;296:1646–7.

17. ten Dijke P, Hill CS. New insights into TGF-β-Smad signalling. Trends Biochem Sci 2004;29:265–73.

18. Rydén M, Imamura T, Jornvall H, et al. A novel type I receptor serine/threonine kinase predominantly expressed in the adult central nervous system. J Biol Chem 1996;271:30603–9.

19. Tsuchida K, Sawchenko PE, Nishikawa SI, Vale WW. Molecular cloning of a novel type I receptor serine/threonine kinase for the TGF-β superfamily from rat brain. Mol Cell Neurosci 1996;7:467–78.

20. Bondestam J, Huotari MA, Moren A, et al. cDNA cloning, expression studies and chromosome mapping of human type I serine/threonine kinase receptor ALK7 (ACVR1C). Cytogenet Cell Genet 2001;95:157–62.

21. Roberts JR, Hu S, Qiu Q, et al. Identification of novel isoforms of activin receptor-like kinase 7 (ALK7) generated by alternative splicing and expression of ALK7 and its ligand, Nodal, in human placenta. Biol Reprod 2003;68:1719–26.

22. Reissmann E, Jornvall H, Blokzijl A, et al. The orphan receptor ALK7 and the activin receptor ALK4 mediate signaling by Nodal proteins during vertebrate development. Genes Dev 2001;15:2010–22.

23. Tsuchida K, Nakatani M, Yamakawa N, Hashimoto O, Hasegawa Y, Sugino H. Activin isoforms signal through type I receptor serine/threonine kinase ALK7. Mol Cell Endocrinol 2004;220:59–65.

24. Jörnvall H, Blokzijl A, ten Dijke P, Ibanez CF. The orphan receptor serine/

threonine kinase ALK7 signals arrest of proliferation and morphological differentiation in a neuronal cell line. J Biol Chem 2001;276:5140–6.

25. Kim BC, Van Gelder H, Kim TA, et al. ALK7 induces apoptosis through activation of MAP kinases in a Smad3-dependent mechanism in hepatoma cells. J Biol Chem 2004;279:28458–65.

26. Munir S, Xu G, Wu Y, Yang BB, Lala K, Peng C. Nodal and activin receptor-like kinase (ALK) 7 inhibit proliferation and induce apoptosis in human trophoblast cells. J Biol Chem 2004;279:31277–86.

27. Debatin K-M. Apoptosis pathways in cancer and cancer therapy. Cancer Immunol Immunother 2004;53:153–9.

28. Schultz DR, Harrington WJ, Jr. Apoptosis: programmed cell death at a molecular level. Semin Arthritis Rheum 2003;32:345–69.

29. Holcik M, Gibson H, Korneluk RG. XIAP: apoptotic brake and promising therapeutic target. Apoptosis 2001;6:253–61.

30. Breckenridge DG, Xue D. Regulation of mitochondrial membrane permeabilization by BCL-2 family proteins and caspases. Curr Opin Cell Biol 2004;16:647–52.

31. Fujita N, Nagahashi A, Nagashima K, Rokudai S, Tsuruo T. Acceleration of apoptotic cell death after the cleavage of Bcl-X_L protein by caspase-3-like proteases. Oncogene 1998;17:1295–304.

32. Rowan S, Fisher DE. Mechanisms of apoptotic cell death. Leukemia 1997; 11:457–65.

33. Suzuki M, Youle RJ, Tjandra N. Structure of Bax: coregulation of dimer formation and intracellular localization. Cell 2000;103:645–54.

34. Fesik AW. Insights into programmed cell death through structural biology. Cell 2000;103:273–82.

35. Yang J, Liu X, Bhalla K, et al. Prevention of apoptosis by Bcl-2: release of cytochrome *c* from mitochondria blocked. Science 1997;275:1129–32.

36. Asselin E, Mills GB, Tsang BK. XIAP regulated Akt activity and caspase-3-depentent cleavage during cisplatin-induced apoptosis in human ovarian epithelial cells. Cancer Res 2001;61:1862–8.

37. Shima Y, Nakao K, Nakashima T, et al. Activation of caspase-8 in transforming growth factor-β-induced apoptosis of human hepatoma cells. Hepatology 1999;30:1215–22.

38. Shooner C, Caron PL, Fréchette-Frigon G, Leblanc V, Déry Dery MC, Asselin E. TGF-β expression during rat pregnancy and activity on decidual cell survival. Reprod Biol Endocrinol 2005;3:20–37.

39. Gottfried Y, Rotem A, Lotan R, Steller H, Larisch S. The mitochondrial ARTS protein promotes apoptosis through targeting XIAP. EMBO J 2004; 23:1627–35.

40. Yamaguchi K, Nagai S, Ninomiya-Tsuji J, et al. XIAP, a cellular member of the inhibitor of apoptosis protein family, links the receptors to TAB1-1 in the BMP signaling pathway. EMBO J 1999;18:179–87.

41. Reffey SB, Wurthner JU, Parks WT, Roberts AB, Duckett CS. X-linked inhibitor of apoptosis protein functions as a cofactor in transforming growth factor-β signaling. J Biol Chem 2001;276:26542–9.

42. Lewis J, Burstein E, Reffey SB, Bratton SB, Roberts AB, Duckett CS. Uncoupling of the signaling and caspase-inhibitory properties of X-linked inhibitor of apoptosis. J Biol Chem 2004;279:9023–9.

43. Yamada SD, Baldwin RL, Karlan BY. Ovarian carcinoma cell cultures are resistant to TGF-β1-mediated growth inhibition despite expression of functional receptors. Gynecol Oncol 1999;75:72–7.

44. Di Simone N, Crowley WF, Jr., Wang QF, Sluss PM, Schneyer AL. Characterization of inhibin/activin subunit, follistatin, and activin type II receptors in human ovarian cancer cell lines: a potential role in autocrine growth regulation. Endocrinology 1996;137:486–94.

45. Choi KC, Kang SK, Nathwani PS, Cheng KW, Auersperg N, Leung PC. Differential expression of activin/inhibin subunit and activin receptor mRNAs in normal and neoplastic ovarian surface epithelium (OSE). Mol Cell Endocrinol 2001;174:99–110.

46. Sánchez-Capelo A. Dual role for TGF-β1 in apoptosis. Cytokine Growth Factor Rev 2005;16:15–34.

47. He TC, Zhou S, da Costa LT, Yu J, Kinzler KW, Vogelstein B. A simplified system for generating recombinant adenoviruses. Proc Natl Acad Sci U S A 1998; 95:2509–14.

48. Xu G, Chakraborty C, Lala PK. Expression of TGF-β signalling genes in the normal, premalignant, and malignant human trophoblast: loss of Smad3 in choriocarcinoma cells. Biochem Biophys Res Commun 2001; 287:47–55.